



Crystal structure and Hirshfeld surface analysis of the salt 2-iodoethylammonium iodide – a possible side product upon synthesis of hybrid perovskites

Hanna R. Petrosova,^{a*} Dina D. Naumova,^a Irina A. Golenya,^a Ildiko Buta^b and Il'ya A. Gural'skiy^a

Received 8 October 2024
Accepted 23 October 2024

Edited by M. Weil, Vienna University of Technology, Austria

Keywords: crystal structure; organic cation; ammonium salt; iodide; hydrogen bonding.

CCDC reference: 2393092

Supporting information: this article has supporting information at journals.iucr.org/e

^aDepartment of Chemistry, Taras Shevchenko National University of Kyiv, Volodymyrska St. 64, Kyiv 01601, Ukraine, and ^b"Coriolan Dragulescu" Institute of Chemistry, Mihai Viteazu Blvd. 24, Timisoara 300223, Romania. *Correspondence e-mail: anna.petrosova@knu.ua

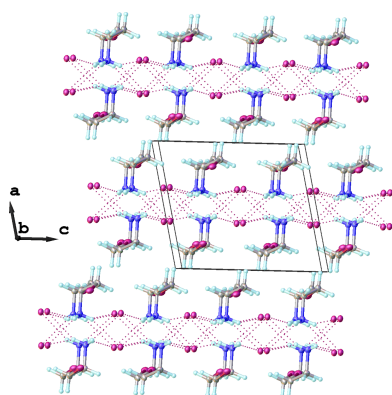
The title organic–inorganic hybrid salt, $C_2H_7IN^+I^-$, is isotypic with its bromine analog, $C_2H_7BrN^+Br^-$ [Semenikhin *et al.* (2024). *Acta Cryst. E* **80**, 738–741]. Its asymmetric unit consists of one 2-iodoethylammonium cation and one iodide anion. The NH_3^+ group of the organic cation forms weak hydrogen bonds with four neighboring iodide anions, leading to the formation of supramolecular layers propagating parallel to the *bc* plane. Hirshfeld surface analysis reveals that the most important contribution to the crystal packing is from $N-H\cdots I$ interactions (63.8%). The crystal under investigation was twinned by a 180° rotation around [001].

1. Chemical context

Hybrid organic–inorganic perovskites are known for their interesting semiconducting and optical properties, which allow their application in photovoltaic and optoelectronic devices (Younis *et al.*, 2021). At the same time, hybrid perovskites create an equally fascinating background for fundamental studies by forming numerous structural motifs of different periodicities.

Even though the structure type *perovskite* usually refers to inorganic compounds with composition ABX_3 (Li *et al.*, 2017), recent developments in this field led to ‘hybrid organic–inorganic perovskites’, which contain discrete or fused $[BX_6]^{n-}$ octahedral building units of inorganic nature, the charge of which is compensated by organic cations. The corresponding octahedra can be connected to each other in various ways, resulting in frameworks with different periodicity (Han *et al.*, 2021).

However, an important issue that demands extra caution upon work with hybrid perovskites is their stability. These materials are very sensitive to water vapor, which can cause their immediate degradation to different products including inorganic salts such as BX_2 and organic salts AX .



Here we report on synthesis and crystal structure of the organic–inorganic hybrid salt 2-iodoethylammonium iodide, $C_2H_7IN^+I^-$. The 2-iodoethylammonium cation has previously been incorporated into some hybrid perovskites with layered arrangements (Xue *et al.*, 2023; Skorokhod *et al.*, 2023). In addition, 2-iodoethylammonium can be formed as a result of

Table 1Hydrogen-bond geometry (\AA , $^\circ$).

$D-H\cdots A$	$D-H$	$H\cdots A$	$D\cdots A$	$D-H\cdots A$
$N1-H1A\cdots I2^i$	0.84	2.74	3.517 (7)	155
$N1-H1B\cdots I2$	0.84	2.85	3.618 (8)	153
$N1-H1C\cdots I2^{ii}$	0.84	2.96	3.627 (8)	139
$N1-H1C\cdots I2^{iii}$	0.84	3.04	3.600 (8)	127

Symmetry codes: (i) $-x+1, -y+1, -z+1$; (ii) $x, -y+\frac{3}{2}, z-\frac{1}{2}$; (iii) $-x+1, y-\frac{1}{2}, -z+\frac{1}{2}$.

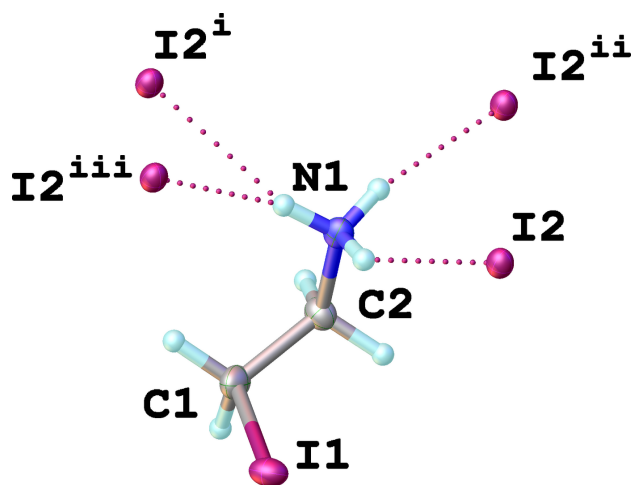
aziridine ring-opening reaction upon synthesis of aziridinium perovskites (Kucheriv *et al.*, 2023; Petrosova *et al.*, 2022). Therefore, the reported structural data of the title compound are valuable for phase analysis, since such a phase can be a side product in the synthesis of hybrid perovskites with 2-iodoethylammonium or aziridinium cations.

2. Structural commentary

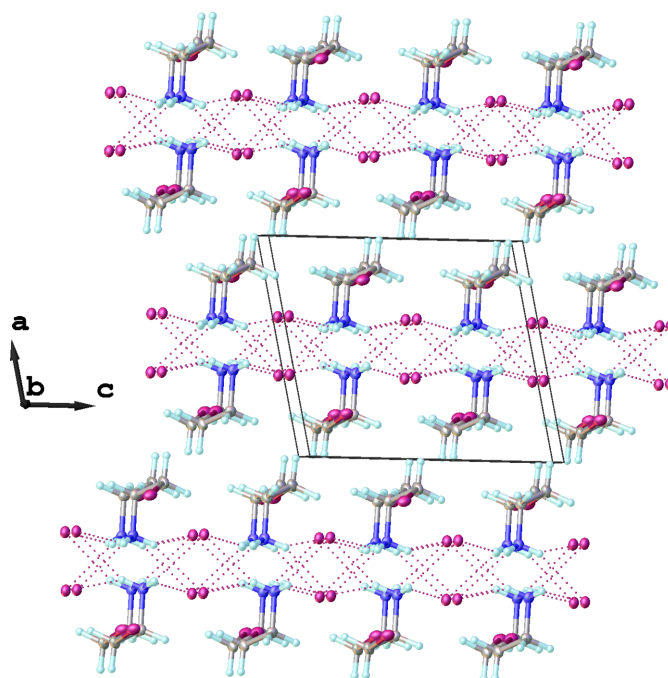
The asymmetric unit consists of one organic 2-iodoethylammonium cation and an iodide counter-ion (Fig. 1). The $I1-C1$ bond length is 2.170 (10) \AA , that of $C1-C2$ is 1.497 (14) \AA and of $C2-N1$ is 1.514 (12) \AA . The torsion angle $I1-C1-C2-N1$ is -65.8 (9) $^\circ$, indicating that the organic cation adopts a synclinal conformation. It is worth noting, that the organic cation $IC_2H_4NH_3^+$ has previously been reported in other crystal structures, but only as a part of hybrid organic-inorganic perovskites (see *Database survey*). The analysis of these structures reveals that this cation can adopt both synclinal and antiperiplanar conformations inside the inorganic frameworks depending on the strength and orientation of the hydrogen bonds formed (Xue *et al.*, 2023).

3. Supramolecular features

Each 2-iodoethylammonium cation is connected to four different iodide anions through weak intermolecular

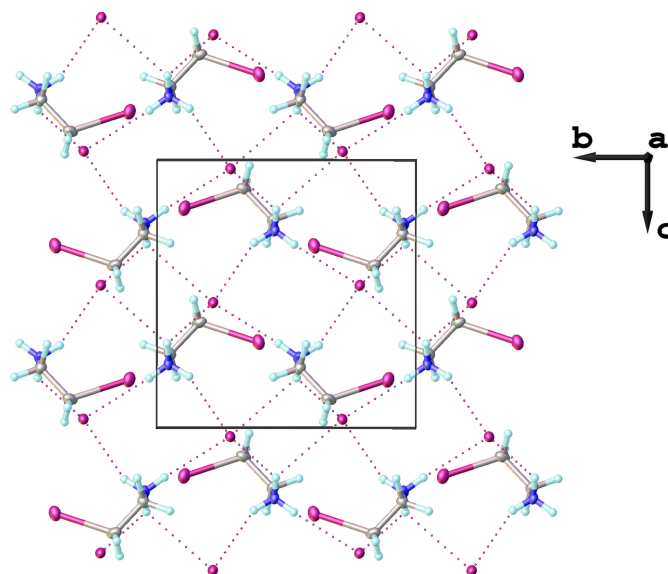
**Figure 1**

The expanded asymmetric unit of the title compound showing hydrogen bonds between the organic cation and iodide anions (dotted lines). Displacement ellipsoids are drawn at the 50% probability level; symmetry codes refer to Table 1.

**Figure 2**

Crystal packing of the title compound in a view approximately along [010] showing infinite supramolecular layers propagating parallel to the bc plane.

$N-H\cdots I$ interactions (Fig. 1). Simultaneously, each iodide anion forms hydrogen bonds with four neighboring $-NH_3^+$ groups of 2-iodoethylammonium cations, forming infinite supramolecular layers propagating parallel to the bc plane (Fig. 2). A view along the a axis of a single supramolecular layer is given in Fig. 3. Numerical parameters of the hydrogen-bonding interactions are compiled in Table 1.

**Figure 3**

A single supramolecular layer viewed along [100].

4. Hirshfeld surface analysis

Hirshfeld surface analysis (Hirshfeld, 1977; Spackman & Jayatilaka, 2009) was used to visualize and quantify intermolecular interactions in 2-iodoethylammonium iodide using *CrystalExplorer* (Spackman *et al.*, 2021). The Hirshfeld surface plotted over d_{norm} and the two-dimensional fingerprint plots are given in Fig. 4. The surface shows the four N—H...I contacts described above as regions colored in red (Fig. 4a), where the color code denotes contacts with distances equal to the sum of the van der Waals radii as white, while those with shorter and longer distances are represented in red and blue, respectively. The two-dimensional fingerprint plots show that the most important interaction found in the structure is represented by N—H...I contacts, which account for 63.8% of all contacts observed in the crystal structure (Fig. 4b). The residual contributions originate from H...H interactions.

5. Database survey

A search in the Cambridge Crystallographic Database (CSD, version 5.45, update of September 2024; Groom *et al.*, 2016) for the 2-iodoethylammonium cation revealed the following structures, which all are based on perovskite-type inorganic anions: JIGYEH, JIGYIL, JIGYUX (Skorokhod *et al.*, 2023); SIWHIQ, TEYMIU (Sourisseau *et al.*, 2007), TEGROQ (Song *et al.*, 2022). The title compound is isotypic with 2-bromoethylammonium bromide (ZOTHAV; Semnikhin *et al.*, 2024).

6. Synthesis and crystallization

All reagents were purchased from UkrOrgSynthet Ltd. and used as received. Aziridine (50 μl) was added to aqueous HI (57% w/w, 300 μl) and was left to crystallize at room temperature. Colorless crystals were harvested after one day and protected under Paratone[®] oil.

Table 2

Experimental details.

Crystal data	
Chemical formula	$\text{C}_2\text{H}_7\text{IN}^+\cdot\text{I}^-$
M_r	298.89
Crystal system, space group	Monoclinic, $P2_1/c$
Temperature (K)	100
a, b, c (\AA)	8.3073 (7), 8.8800 (6), 9.3838 (7)
β ($^\circ$)	102.004 (7)
V (\AA^3)	677.10 (9)
Z	4
Radiation type	Mo $K\alpha$
μ (mm^{-1})	9.16
Crystal size (mm)	$0.31 \times 0.15 \times 0.07$
Data collection	
Diffractometer	XtaLAB Synergy, Dualflex, HyPix Analytical (<i>CrysAlis PRO</i> ; Rigaku OD, 2023)
Absorption correction	
$T_{\text{min}}, T_{\text{max}}$	0.157, 0.573
No. of measured, independent and observed [$I > 2\sigma(I)$] reflections	2744, 2744, 2535
$(\sin \theta/\lambda)_{\text{max}}$ (\AA^{-1})	0.712
Refinement	
$R[F^2 > 2\sigma(F^2)], wR(F^2), S$	0.051, 0.159, 1.12
No. of reflections	2744
No. of parameters	49
H-atom treatment	H atoms treated by a mixture of independent and constrained refinement
$\Delta\rho_{\text{max}}, \Delta\rho_{\text{min}}$ (e \AA^{-3})	2.07, -1.68

Computer programs: *CrysAlis PRO* (Rigaku OD, 2023), *SHELXT* (Sheldrick, 2015a), *SHELXL* (Sheldrick, 2015b), *OLEX2* (Dolomanov *et al.*, 2009) and *publCIF* (Westrip, 2010).

7. Refinement

Crystal data, data collection and structure refinement details are summarized in Table 2. The crystal under investigation was twinned by a 180° rotation around [001] and the intensity data processed into a HKLF5-type file; the twin components refined to a ratio of 0.617 (2):0.383 (2). Hydrogen atoms were placed at calculated positions with $U_{\text{iso}}(\text{H}) = 1.2U_{\text{eq}}(\text{C})$ and $U_{\text{iso}}(\text{H}) = 1.5U_{\text{eq}}(\text{N})$.

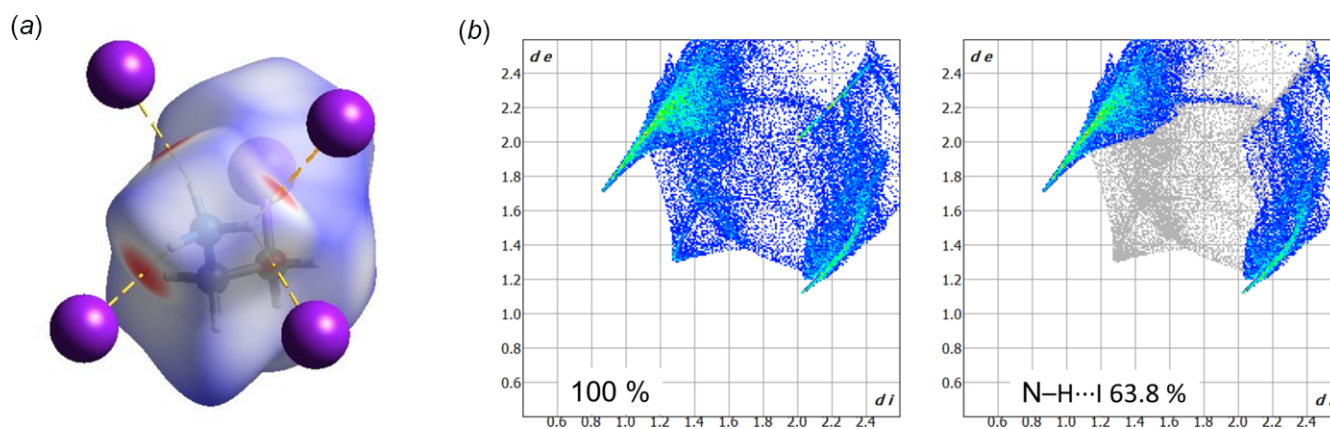


Figure 4

(a) Hirshfeld surface of the 2-iodoethylammonium cation plotted over d_{norm} , showing the strongest interactions with I^- anions (in red); (b) the two-dimensional fingerprint plots for 2-iodoethylammonium iodide (left) and delineated into N—H...I contacts (right).

Funding information

Funding for this research was provided by: Ministry of Education and Science of Ukraine (grant Nos. 24BF037-02 and 24BF037-01M).

References

- Dolomanov, O. V., Bourhis, L. J., Gildea, R. J., Howard, J. A. K. & Puschmann, H. (2009). *J. Appl. Cryst.* **42**, 339–341.
- Groom, C. R., Bruno, I. J., Lightfoot, M. P. & Ward, S. C. (2016). *Acta Cryst.* **B72**, 171–179.
- Han, Y., Yue, S. & Cui, B. (2021). *Adv. Sci.* **8**, 2004805.
- Hirshfeld, H. L. (1977). *Theor. Chim. Acta*, **44**, 129–138.
- Kucheriv, O. I., Sirenko, V. Y., Petrosova, H. R., Pavlenko, V. A., Shova, S. & Gural'skiy, I. A. (2023). *Inorg. Chem. Front.* **10**, 6953–6963.
- Li, W., Wang, Z., Deschler, F., Gao, S., Friend, R. H. & Cheetham, A. K. (2017). *Nat. Rev. Mater.* **2**, 16099.
- Petrosova, H. R., Kucheriv, O. I., Shova, S. & Gural'skiy, I. A. (2022). *Chem. Commun.* **58**, 5745–5748.
- Rigaku OD (2023). *CrysAlis PRO*. Rigaku Oxford Diffraction, Yarnton, England.
- Semenikhin, O. A., Shova, S., Golenya, I. A., Naumova, D. D. & Gural'skiy, I. A. (2024). *Acta Cryst.* **E80**, 738–741.
- Sheldrick, G. M. (2015a). *Acta Cryst.* **A71**, 3–8.
- Sheldrick, G. M. (2015b). *Acta Cryst.* **C71**, 3–8.
- Skorokhod, A., Quarti, C., Abhervé, A., Allain, M., Even, J., Katan, C. & Mercier, N. (2023). *Chem. Mater.* **35**, 2873–2883.
- Song, Z., Yu, B., Wei, J., Li, C., Liu, G. & Dang, Y. (2022). *Inorg. Chem.* **61**, 6943–6952.
- Sourisseau, S., Louvain, N., Bi, W., Mercier, N., Rondeau, D., Buzaré, J.-Y. & Legein, C. (2007). *Inorg. Chem.* **46**, 6148–6154.
- Spackman, M. A. & Jayatilaka, D. (2009). *CrystEngComm*, **11**, 19–32.
- Spackman, P. R., Turner, M. J., McKinnon, J. J., Wolff, S. K., Grimwood, D. J., Jayatilaka, D. & Spackman, M. A. (2021). *J. Appl. Cryst.* **54**, 1006–1011.
- Westrip, S. P. (2010). *J. Appl. Cryst.* **43**, 920–925.
- Xue, J., Huang, Y., Liu, Y., Chen, Z., Sung, H. H. Y., Williams, I. D., Zhu, Z., Mao, L., Chen, X. & Lu, H. (2023). *Angew. Chem. Int. Ed.* **62**, e202304486.
- Younis, A., Lin, C., Guan, X., Shahrokhi, S., Huang, C., Wang, Y., He, T., Singh, S., Hu, L., Retamal, J. R. D., He, J. & Wu, T. (2021). *Adv. Mater.* **33**, 2005000.

supporting information

Acta Cryst. (2024). E80, 1226-1229 [https://doi.org/10.1107/S205698902401034X]

Crystal structure and Hirshfeld surface analysis of the salt 2-iodoethylammonium iodide – a possible side product upon synthesis of hybrid perovskites

Hanna R. Petrosova, Dina D. Naumova, Irina A. Golenya, Ildiko Buta and Il'ya A. Gural'skiy

Computing details

2-Iodoethylammonium iodide

Crystal data

$C_2H_7IN^+I^-$

$M_r = 298.89$

Monoclinic, $P2_1/c$

$a = 8.3073$ (7) Å

$b = 8.8800$ (6) Å

$c = 9.3838$ (7) Å

$\beta = 102.004$ (7)°

$V = 677.10$ (9) Å³

$Z = 4$

$F(000) = 528$

$D_x = 2.932$ Mg m⁻³

Mo $K\alpha$ radiation, $\lambda = 0.71073$ Å

Cell parameters from 3490 reflections

$\theta = 3.2$ – 30.3 °

$\mu = 9.16$ mm⁻¹

$T = 100$ K

Plate, clear intense colourless

$0.31 \times 0.14 \times 0.07$ mm

Data collection

XtaLAB Synergy, Dualflex, HyPix
diffractometer

Detector resolution: 10.0000 pixels mm⁻¹

ω scans

Absorption correction: analytical
(CrysAlisPro; Rigaku OD, 2023)

$T_{\min} = 0.157$, $T_{\max} = 0.573$

2744 measured reflections

2744 independent reflections

2535 reflections with $I > 2\sigma(I)$

$\theta_{\max} = 30.4$ °, $\theta_{\min} = 2.5$ °

$h = -11 \rightarrow 10$

$k = -11 \rightarrow 11$

$l = -10 \rightarrow 12$

Refinement

Refinement on F^2

Least-squares matrix: full

$R[F^2 > 2\sigma(F^2)] = 0.051$

$wR(F^2) = 0.159$

$S = 1.12$

2744 reflections

49 parameters

0 restraints

Hydrogen site location: inferred from
neighbouring sites

H atoms treated by a mixture of independent
and constrained refinement

$w = 1/[\sigma^2(F_o^2) + (0.1098P)^2 + 4.1089P]$

where $P = (F_o^2 + 2F_c^2)/3$

$(\Delta/\sigma)_{\max} < 0.001$

$\Delta\rho_{\max} = 2.07$ e Å⁻³

$\Delta\rho_{\min} = -1.68$ e Å⁻³

Special details

Geometry. All esds (except the esd in the dihedral angle between two l.s. planes) are estimated using the full covariance matrix. The cell esds are taken into account individually in the estimation of esds in distances, angles and torsion angles; correlations between esds in cell parameters are only used when they are defined by crystal symmetry. An approximate (isotropic) treatment of cell esds is used for estimating esds involving l.s. planes.

Refinement. Refined as a 2-component twin.

Fractional atomic coordinates and isotropic or equivalent isotropic displacement parameters (\AA^2)

	<i>x</i>	<i>y</i>	<i>z</i>	$U_{\text{iso}}^*/U_{\text{eq}}$
I2	0.63381 (7)	0.78334 (6)	0.53313 (6)	0.0165 (2)
I1	0.19546 (8)	0.89307 (7)	0.17832 (7)	0.0224 (2)
N1	0.3819 (10)	0.5459 (8)	0.2618 (8)	0.0176 (15)
H1A	0.412 (3)	0.471 (7)	0.314 (7)	0.026*
H1B	0.417 (3)	0.624 (7)	0.307 (8)	0.026*
H1C	0.419 (3)	0.540 (8)	0.186 (6)	0.026*
C2	0.1958 (12)	0.5506 (11)	0.2219 (10)	0.0200 (18)
H2A	0.153639	0.449803	0.187631	0.024*
H2B	0.152455	0.575673	0.309573	0.024*
C1	0.1349 (13)	0.6643 (12)	0.1053 (10)	0.024 (2)
H1D	0.013934	0.654792	0.073950	0.028*
H1E	0.183992	0.642845	0.019956	0.028*

Atomic displacement parameters (\AA^2)

	U^{11}	U^{22}	U^{33}	U^{12}	U^{13}	U^{23}
I2	0.0214 (4)	0.0135 (4)	0.0150 (4)	−0.00033 (17)	0.0051 (3)	0.00083 (17)
I1	0.0189 (4)	0.0192 (4)	0.0301 (4)	0.0035 (2)	0.0068 (3)	0.0037 (2)
N1	0.022 (4)	0.013 (3)	0.019 (4)	−0.002 (3)	0.006 (3)	0.001 (3)
C2	0.020 (4)	0.020 (5)	0.020 (5)	−0.001 (3)	0.003 (4)	0.003 (3)
C1	0.024 (5)	0.029 (5)	0.017 (4)	0.004 (4)	0.001 (4)	−0.005 (4)

Geometric parameters (\AA , $^\circ$)

I1—C1	2.170 (10)	C2—H2A	0.9900
N1—H1A	0.84 (6)	C2—H2B	0.9900
N1—H1B	0.84 (6)	C2—C1	1.497 (14)
N1—H1C	0.84 (6)	C1—H1D	0.9900
N1—C2	1.514 (12)	C1—H1E	0.9900
H1A—N1—H1B	109.5	C1—C2—N1	111.9 (8)
H1A—N1—H1C	109.5	C1—C2—H2A	109.2
H1B—N1—H1C	109.5	C1—C2—H2B	109.2
C2—N1—H1A	109.5	I1—C1—H1D	109.1
C2—N1—H1B	109.5	I1—C1—H1E	109.1
C2—N1—H1C	109.5	C2—C1—I1	112.3 (6)
N1—C2—H2A	109.2	C2—C1—H1D	109.1
N1—C2—H2B	109.2	C2—C1—H1E	109.1

H2A—C2—H2B	107.9	H1D—C1—H1E	107.9
N1—C2—C1—I1	-65.8 (9)		

Hydrogen-bond geometry (Å, °)

<i>D</i> —H··· <i>A</i>	<i>D</i> —H	H··· <i>A</i>	<i>D</i> ··· <i>A</i>	<i>D</i> —H··· <i>A</i>
N1—H1A···I2 ⁱ	0.84	2.74	3.517 (7)	155
N1—H1B···I2	0.84	2.85	3.618 (8)	153
N1—H1C···I2 ⁱⁱ	0.84	2.96	3.627 (8)	139
N1—H1C···I2 ⁱⁱⁱ	0.84	3.04	3.600 (8)	127

Symmetry codes: (i) $-x+1, -y+1, -z+1$; (ii) $x, -y+3/2, z-1/2$; (iii) $-x+1, y-1/2, -z+1/2$.